Title

Printable Ultrathin Metal Oxide Semiconductor-Based Conformal Biosensors

Journal

ACS Nano, 9(12)

ISSN

1936-0851

Authors

Rim, You Seung

Bae, Sang-Hoon

Chen, Huajun

et al.

Publication Date

2015-12-22

DOI

10.1021/acsnano.5b05325

Peer reviewed

Printable Ultrathin Metal Oxide Semiconductor-Based Conformal Biosensors

You Seung Rim,[*,†,‡,#] Sang-Hoon Bae,[†,‡,#] Huajun Chen,[†,‡] Jonathan L. Yang,[†,§] Jaemyung Kim,[†,∥] Anne M. Andrews,[∥,⊥] Paul S. Weiss,[†,‡,∥] Yang Yang,[†,‡] and Hsian-Rong Tseng[*,†,§]

[†]California NanoSystems Institute, [‡]Department of Materials Science and Engineering, [§]Department of Pharmacology, [∥]Department of Chemistry and Biochemistry, and [⊥]Department of Psychiatry, Hatos Center for Neuropharmacology, and Semel Institute for Neuroscience and Human Behavior, University of California, Los Angeles, Los Angeles, California 90095, United States. [#]These authors contributed equally.

ABSTRACT Conformal bioelectronics enable wearable, noninvasive, and health-monitoring platforms. We demonstrate a simple and straightforward method for producing thin, sensitive In_2O_3-based conformal biosensors based on field-effect transistors using facile solution-based processing. One-step coating *via* aqueous In_2O_3 solution resulted in ultrathin (3.5 nm), high-density, uniform films over large areas. Conformal In_2O_3-based biosensors on ultrathin polyimide films displayed good device performance, low mechanical stress, and highly conformal contact determined using polydimethylsiloxane artificial skin having complex curvilinear surfaces or an artificial eye. Immobilized In_2O_3 field-effect transistors with self-assembled monolayers of NH_2-terminated silanes functioned as pH sensors. Functionalization with glucose oxidase enabled D-glucose detection at physiologically relevant levels. The conformal ultrathin field-effect transistor biosensors developed here offer new opportunities for future wearable human technologies.

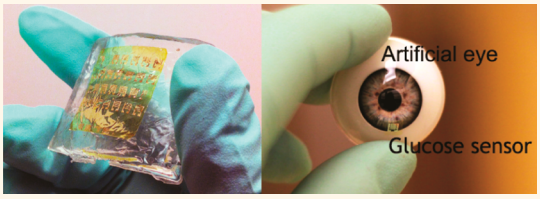

KEYWORDS: biosensor · aqueous process · metal oxide semiconductor · conformal · flexible · field-effect transistor

The development of wearable sensors for *in situ*, rapid, and low-cost detection of biologically and medically important targets (*e.g.*, heart rate and glucose levels) that are lightweight, comfortable, and small scale will be useful for many applications involving electronic skin, diagnosis, thermal regulation, and communication.[1−14] Depending on the specific applications, nanomaterials including nanowires, nanosheets, and nanoparticles made of inorganic or organic materials have been used because of their high sensitivity and flexibility.[3,15−24] Considering the functional nanostructures used in biosensors, the selection of the detection platform is critical to high sensitivity and reproducibility, including low detection limits, low device-to-device variation, real-time detection, and simple integration with wearable environments (*e.g.*, human skin, clothes, and flexible or rollable electronic devices). Field-effect transistor (FET)-based biosensors are well suited to detecting biomolecules because the exposed semiconductor channel regions can be chemically modified with high-sensitivity functional groups or receptors.[25−28] Specific interactions between receptor groups and their targets alter local electric fields causing variations in channel conductance even at low target concentrations. This control can be due to conformational changes upon recognition in the receptors that are held close to the active element or by displacing environmental charges with neutral, less charged, or oppositely charged components of the receptors.[27] One-dimensional (1D) and two-dimensional (2D) nanomaterials such as Si nanowires (SiNWs), carbon nanotubes (CNTs), graphene, and In_2O_3 or MoS_2 thin-films have been employed as channel materials for FET platforms because of their large surface-to-volume ratios and similar electric potentials of the surface and bulk, thus providing high sensitivity responses.[26,27,29−32]

The major challenges of using nanomaterials for FET-based wearable biosensors are obtaining both the required conformality and reproducibility.[4,10,18,33] Highly conformal contact of devices on curvilinear, complex surface topologies of biological tissues, skin,

* Address correspondence to ysrim79@ucla.edu, hrtseng@mednet.ucla.edu.

Received for review August 25, 2015 and accepted October 25, 2015.

Published online October 25, 2015
10.1021/acsnano.5b05325

electronic devices, and unknown targets is a key feature.[1] Several approaches have been taken to address issues associated with curvilinear and/or irregular surfaces such as using silk fibroin or ultrathin polyethylene terephthalate (PET), and transferring devices by an exfoliating method.[7,21−23,34] Reproducibility is highly related to the material systems, including 1D and 2D growth and integration on devices, and is essential to controlling densities and alignment to obtain electrical uniformity through complex processing. Although these approaches have been significantly improved for realizing conformal and highly sensitive devices, complex processing and materials have been considered in order to address reproducibility. Consequently, simple and large-scale applications of biosensor platforms are highly desirable. To overcome these issues, we proposed and demonstrated sensor arrays based on solution-processed metal oxide semiconductors *via* simple chemistry with low impurity levels, which are effective for the fabrication of ultrathin films.[27] Simple spin-coating of indium oxide solution formed ultrathin films (~3.5 nm) with high film density. Ultrathin films can avoid the intrinsic effects of strain such as physical strain and peeling from substrates.[10,11,35] Furthermore, oxide surfaces can be straightforwardly chemical functionalized with biochemical moieties.

Here, we advance this strategy to produce highly sensitive, conformal biosensors that can be used for noninvasive health monitoring and are wearable, compared with our previous dopamine sensors on rigid substrates.[27] Two applications are demonstrated initially on artificial skin and eye replicas: measurements of pH and glucose levels. These proposed health-monitoring platforms not only permitted straightforward processing of sensor-arrays for high flexibility and conformality but also had simple routes for chemically functionalizing the semiconductor surfaces.[36,37] The pH levels in the human body can change in response to physiologic conditions such as tumorigenesis.[38] Local pH values not only provide important information for drug delivery but also reflect health problems directly.[39] Moreover, blood glucose levels are altered in patients with diabetes mellitus. Currently, regular monitoring requires the use of invasive finger-stick tests to determine blood glucose levels.[40] A noninvasive test for glucose levels in tears is challenging to develop because of the need for glucose detection limits in the range of 0.1−0.6 mM, which is lower than glucose concentrations in blood (2−30 mM in diabetics).[41−43]

RESULTS AND DISCUSSION

We developed ultrathin (3.5 nm) and highly uniform indium oxide (In_2O_3) semiconductors *via* a single spin-coating step using hexaaqua metal(III) complexes and annealing at low temperature (250 °C).[27] Oxide semiconductors that are a few nanometers thick have high surface sensitivities and reactivities with specific molecular assemblies that are advantageous for detecting specific analytes. Simple and fast removal of conformal films from underlying substrates is well suited to wearable biosensor applications.[27] Ultrathin In_2O_3 semiconductors were mechanically stable following removal from substrates. By combining ultrathin In_2O_3 semiconductor-based FETs with conformal films, we produced highly sensitive, easily processed, economical, and conformal biosensors that detected pH values and D-glucose concentrations with physiologically relevant detection limits.

The In_2O_3 films were formed from an aqueous precursor. Resulting films had high densities and were ultrathin and smooth. Film densities were calculated by nondestructive X-ray reflectivity measurements and simulation, which indicated a density of 5.852 $g \cdot cm^{-3}$ (Figure 1a). Compared to single-crystal In_2O_3, the film had high density even after the 250 °C annealing process. Spin-coating of In_2O_3 solutions formed 35 Å-thick films, which were verified by discrete Fourier-transform (DFT) simulation (Figure 1b). Furthermore, In_2O_3 films had smooth surfaces with a root-mean-square (RMS) roughness of 1.1 nm (Figure 1c).

Simple and facile processing of In_2O_3 semiconductor-based FETs was then carried out (Figure 1d). Typically, solution-processed metal-oxide FETs have poor electrical performance when fabricated *via* low-temperature processes.[44,45] The devices produced here, however, showed high saturation mobilities (μ_{sat}), large on/off ratios, and good switching behavior. We attribute these superior performance characteristics to the use of the nitrate-ligand-based hexaaqua indium(III) cation ($[In(H_2O)_6]^{3+}$), which easily decomposed at low temperature to form high-density In_2O_3 films without organic residues, compared to conventional methods.[27,45,46] Hexaaqua indium(III) cations were a key component to realizing high-performance In_2O_3 FETs. Saturation mobilities exceeded ~20 $cm^2 \cdot V^{-1} \cdot s^{-1}$ with on/off ratios over 10^7 (Figure 1e). The gate-to-source leakage current (I_{GS}, gray line) was below 100 pA. Output curves of In_2O_3 FETs induced gate voltages between 0 and 40 V (Figure 1f).

We tested and confirmed that the ultrathin In_2O_3 FETs had good electrical performance after low-temperature processing. To realize pH- and glucose-sensing using flexible transistor platforms, we fabricated ultrathin polyimide (PI) films (2 μm) on glass substrates followed by aqueous processing of In_2O_3 FETs with interdigitating electrodes (Figure 2a). Interdigitated electrodes generate strong electric fields and show low current crowding effects. Fabricated devices were carefully delaminated under water, and the hydrophobic PI films were easily stretched and floated in water. Finally, the devices were transferred onto artificial polydimethylsiloxane (PDMS) skin replicas having highly random surface structures. The ultrathin PI films conformably contacted the artificial skin surfaces *via*

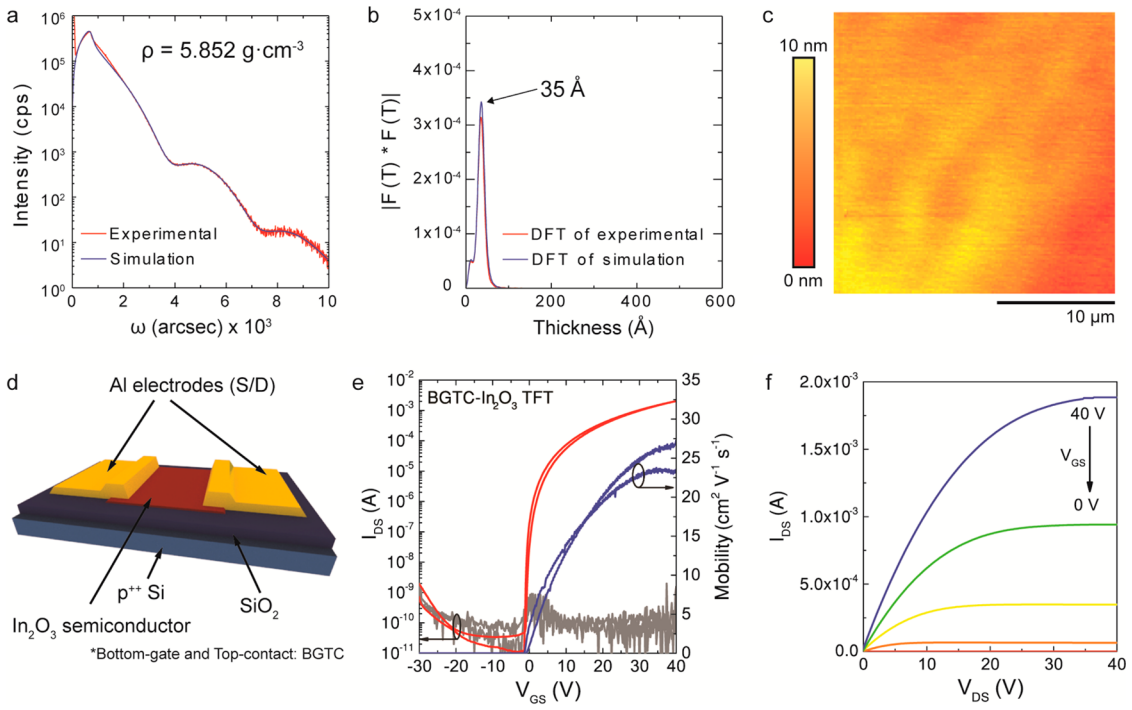

Figure 1. Ultrathin solution-processed In_2O_3 films and associated FETs. (a) X-ray reflectivity of an In_2O_3 thin-film. The film density was 5.582 g·cm^{-3} (82% of the single crystal density of 7.12 g·cm^{-3}). (b) DFT simulation was performed to obtain the precise thickness of In_2O_3 films (35 Å) based on XRR measurements. (c) An atomic force microscopy image of a 35 Å-thick In_2O_3 film. The root-mean-square value is 1.1 nm. (d−f) Schematic of the device structure and electrical performance of In_2O_3 FETs. The overall device structure was BGTC. The BGTC-In_2O_3 FETs performed well with a μ_{sat} of 24.4 ± 2.1 cm^2·V^{-1}·s^{-1}, $I_{on/off}$ of ~10^8, and a subthreshold voltage swing (S. S) of 0.58 ± 0.1 V·dec^{-1}. Output curves showed good pinch-off behavior.

van der Waals forces.[47] We demonstrated conformal contacted devices on human skin and an artificial eye (Figure 2b). Glucose levels can be detected in tears, urine, saliva, and blood; however, tear glucose levels are lower than in blood and urine.[43] To develop artificial contact lens glucose sensors,[41] these differences in detection ranges need to be addressed (*vide infra*). We confirmed that conformally contacted films exhibited good adhesion, regardless of relaxation and tension of the hand. The performance of liquid-gated In_2O_3 FETs on rigid and skin-replica PDMS is shown in Figure 2c,d. Ultrathin In_2O_3 deposited on thin PI films had small strain values when the devices were delaminated from the glass substrates. Furthermore, the devices did not deteriorate on artificial PDMS skin samples with rough surfaces. The In_2O_3 FETs had good pinch-off behavior and low voltage driving with low leakage currents between the Au electrodes and the electrolyte. The latter avoids redox reactions between gate-source electrodes and target molecules in phosphate-buffered saline (PBS) solutions (Figures S1 and S2). Although we confirmed low leakage currents of these devices, implanted electronic devices face safety challenges due to possible leakage current due to the lack of grounding electrodes and circuit passivation. Leakage currents can cause fatal damage to the heart tissue, for example, in ionic biologic fluids.[48] To avoid electrical shock and tissue/organ hazards, further work may be needed to improve insulation and/or isolation in such devices before they would be appropriate for internal/implantable use.

For a more detailed analysis of conformal contact, we investigated adhesion energies between devices and target substrates. The critical adhesion energy for conformal contact was calculated enabling a prediction of the maximal device thickness that would enable conformal contact.[1,35] The surface roughness of target substrates was used to define the numerical model (Figure S3). Since the adhesion energy depends strongly on the bending stiffness of devices, stiffness was first calculated based on the mechanical properties of the devices and target substrates (Figure 3a). Based on the calculated bending stiffness values, we further investigated the relationship between adhesion energy and device thickness with respect to conformal contact. Based on the surface profile, we derived a overlapping two-cylinder model for the numerical modeling of adhesion energy. Since the required adhesion energy in a wet state for conformal contact is 10 mJ·m^{-2}, as described previously,[49] the critical adhesion energy should be less than the required adhesion energy. Thus, the adhesion energy can be calculated as

$$\gamma = \frac{EI}{2R^2b}\{1 + (1+\lambda)R^2/(1-\lambda)r^2\} \qquad (1)$$

where γ, EI, R, b, λ, and r are the calculated adhesion energy, device stiffness, radius of the model cylinders,

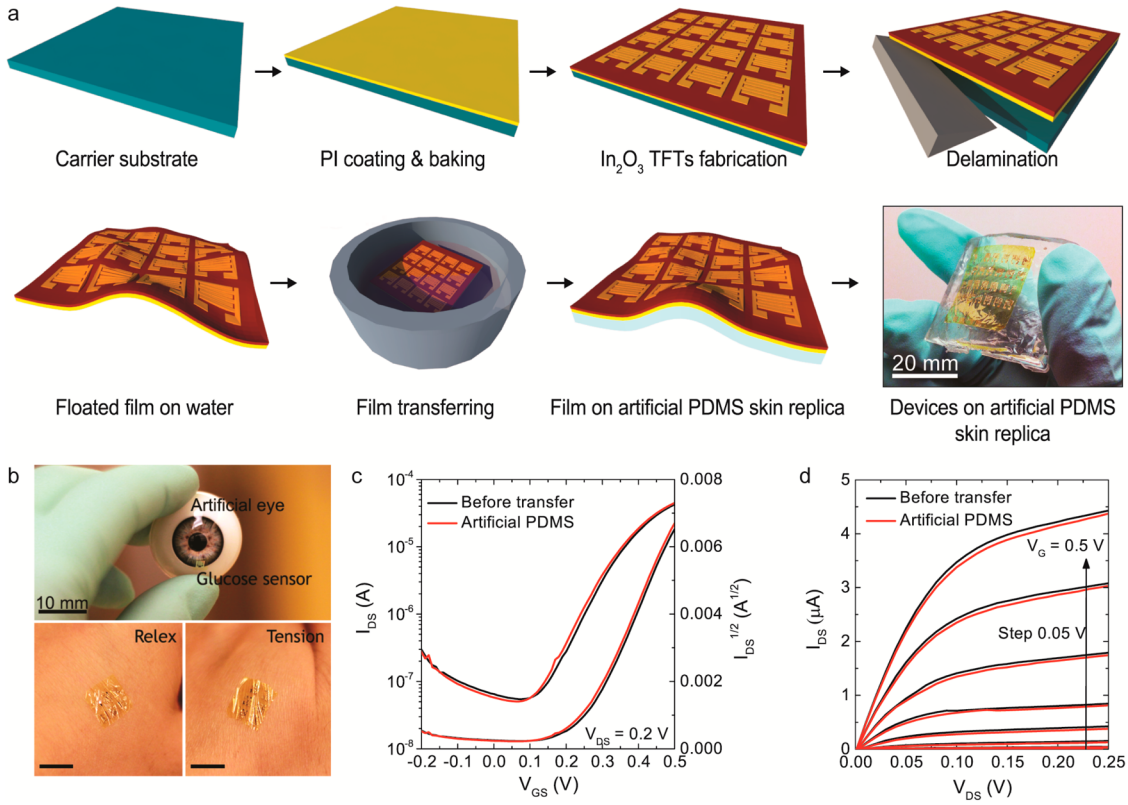

Figure 2. Liquid-gated In_2O_3 FET-based conformal biosensors. (a) Schematic illustration of the flexible biosensor fabrication procedure. Glass substrates were coated with a thin film of PI. Next, In_2O_3 thin-films were deposited over PI *via* an aqueous solution-phase spin-coating procedure. The In_2O_3 thin-films were then annealed at 250 °C. Interdigitating Au/Cr electrodes were patterned by photolithography. The PI films with In_2O_3 FET arrays were delaminated from the underlying glass substrates and floated in water to unroll the films. Artificial PDMS skin replicas were prepared. Thin-film In_2O_3 FET sensors were transferred to artificial PDMS skin samples. Ultrathin PI films easily contacted uneven artificial skin surfaces. (b) Conceptual images of conformally contacted devices on an artificial eye for glucose sensing in tears are shown. Thin-film sensors remained in contact with skin even during tension and relaxation. (c,d) Device performance of thin-film In_2O_3 FETs on rigid substrates and flexible artificial PDMS skin substrates is shown. After transfer of In_2O_3 FETs to skin replicas, devices had similar performance under liquid gating with 1× PBS solution. Low voltage driving and good pinch-off characteristics were observed.

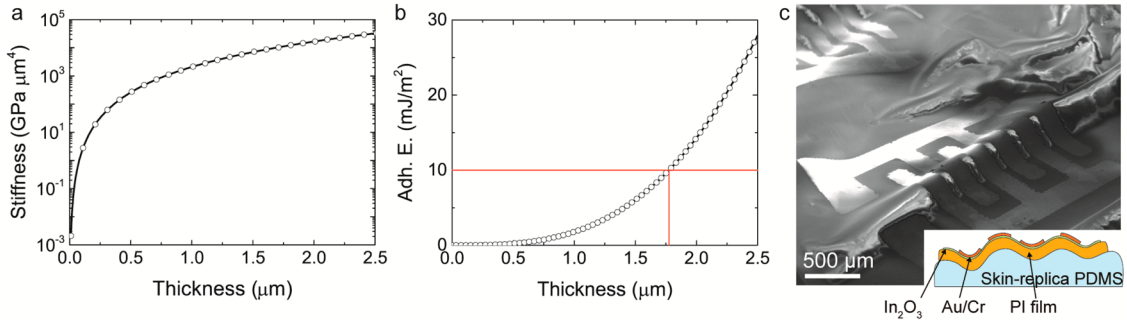

Figure 3. Mechanical modeling and conformal contact of thin-film In_2O_3 FET devices on artificial PDMS skin. (a) Device stiffness calculated as a function of thickness. (b) Adhesion energy values calculated as a function of device thickness indicating the critical thickness for conformal contact. The intersection of the red lines shows the maximal device thickness needed to make conformal contact with PDMS rough substrates. (c) Scanning electron microscope image of a representative device (thickness ~1.7 μm) on an artificial PDMS skin replica indicating conformal contact between the device and the substrate.

the device width, wavelength, and the arc between overlapped cylinders, respectively. Spontaneous and conformal contact begins to occur at a thickness of 1.77 μm, the critical device thickness (Figure 3b), which indicates that conformal contact between the devices and the target substrates happens once each device has a thickness less than the critical thickness. We successfully demonstrated conformal contact between the devices (thickness ~1.7 μm) and PDMS skin replicas (Figure 3b). To evaluate the flexibility of the In_2O_3-based biosensors, we calculated the mechanical strain of the In_2O_3 films on artificial PDMS skin replicas for the

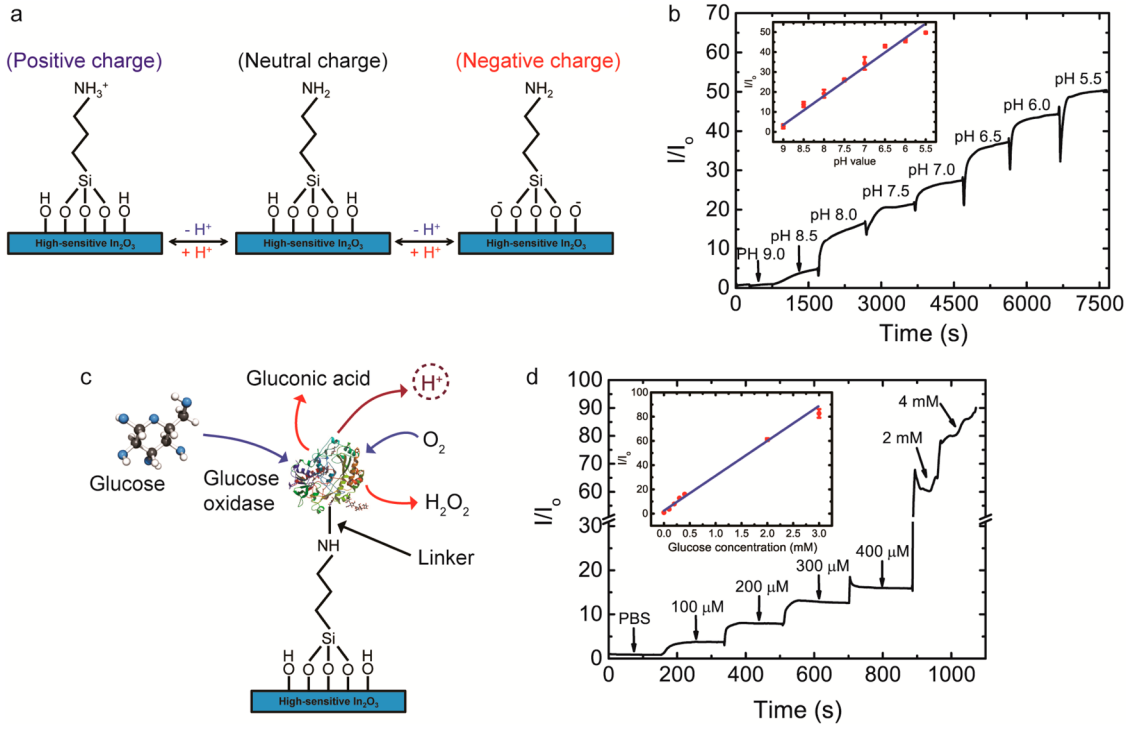

Figure 4. Chemical sensing *via* In_2O_3 FET-based conformal biosensors. (a) The pH-sensing mechanism occurs by protonation of In_2O_3 surface hydroxyl groups and primary amines of APTES at decreasing pH (increasing proton concentrations). (b) Representative responses of an In_2O_3-based FET biosensor to a biologically important pH range (pH 5.5−9). Inset shows data from five devices. (c) Enzymatic oxidation of D-glucose *via* glucose oxidase to produce gluconic acid and hydrogen peroxide. Protons are generated during this oxidation and protonation of the In_2O_3 surfaces is manifested. (d) Representative responses of In_2O_3 sensors to physiologically relevant D-glucose concentrations found in human diabetic tears (lower range) and blood (upper range). Inset shows data from five devices. Error bars represent standard deviations of the means.

overall bending radius of 837 μm (see Supporting Information). The calculated strain value of the In_2O_3 films was 0.078−0.082%. Typically, the electrical and structural properties of In-base oxide films do not change at the strain of below 1%.[50−55] Thus, these values do not affect the electrical degradation of In_2O_3 films even at a small bending radius of below 1 mm.

Figure 4a shows a schematic for pH sensing using the ultrathin In_2O_3 FET-based biosensors developed here *via* a liquid gate setup. Prior to using FETs for pH sensing, In_2O_3 surfaces were silanized using amine-terminated (3-aminopropyl)triethoxysilane (APTES). A representative plot of the drain current response (I/I_o) *vs* pH shows that the response linearly decreases from pH 5.5 to pH 9.0 (Figure 4b). The drain current response eventually saturates at each pH. When pH is increased, the signal increases rapidly and gradually saturates (Figure S4). Thus, saturated values can be used to detect each pH. The linear pH response occurred at a rate of 8.6 ± 0.4 μA/pH unit originating from the deprotonation of APTES amine groups.[56] As shown in Figure S4, the slow saturation response of the drain current is still a challenge for the rapid detecting systems, and further studies of improved response time in these sensor platforms are required.

The silanized In_2O_3 surfaces had better pH sensitivity than unsilanized In_2O_3 FETs due to the APTES terminal amino groups added to the surfaces of the In_2O_3 films (Figure S5). Noise levels of the devices without APTES were also higher than for devices with APTES. Moreover, unfunctionalized devices exhibited nonlinear behavior over the pH range tested compared to devices with APTES silanization. We posit that acquisition of positive charge due to protonation of surface amine groups alters local FET electric fields causing changes in conductance and, thus, current. This behavior is attributed to variations in surface charge densities. Typically, the H^+ concentration depends exponentially on pH values. We therefore predicted that current levels would similarly change exponentially for our devices.[18] Nonetheless, a linear response in pH variations was observed. The response of sensors vary linearly with pH of solution was observed with functionalized amide and OH groups on the surface.[18,57]

To test our devices in a different chemical sensing application, In_2O_3-thin-film FET biosensors were used to detect D-glucose. Glucose sensing was based on the oxidation of D-glucose by the enzyme glucose oxidase (Figure 4c). Typically, previous glucose sensors are based on measuring changes in hydrogen, oxygen, or hydrogen peroxide levels resulting from the enzymatic production of gluconic acid.[58] We explored the

protonation of In_2O_3 surfaces through enzymatic oxidation of D-glucose with glucose oxidase as follows:[59−61]

$$D\text{-glucose} + O_2 + H_2O \xrightarrow[\text{glucose oxidase}]{} \text{gluconic acid} + H^+ + H_2O_2 \quad (2)$$

The production of H^+ depends on the concentration of D-glucose, which alters the pH of PBS solution.[61] Figure 3d shows representative responses of flexible In_2O_3 thin-film FET biosensors acquired upon addition of different glucose concentrations. As D-glucose was increased from 100 to 400 μM (the range expected in diabetic human tears),[41] changes in current responses were detected. Responses showed linear and saturating behavior. Moreover, higher concentrations of D-glucose such as those found in blood from diabetic individuals (*i.e.*, 2 and 4 mM) were also detected with the same linear relationship as the lower D-glucose concentrations. Thus, these In_2O_3-based FET biosensors are compatible for sensing over a wide range of physiological glucose concentrations. To test substrate selectivity, we tested L-glucose over the concentration range from 100 μM to 1 mM. L-Glucose is an enantiomer of D-glucose, and glucose oxidase recognizes only D-glucose. As expected, sensors did not respond to L-glucose (Figure S6).[62]

CONCLUSIONS AND PROSPECTS

In summary, we developed a simple solution-processing procedure for fabricating ultrathin, sensitive In_2O_3 semiconductor-based FETs for use as chemical biosensors. One-step spin-coating of aqueous In_2O_3 solutions formed nanometer-thick (3.5 nm), smooth and highly uniform films over large fabrication areas. The In_2O_3-based FETs had mobilities of $\sim$20 $cm^2 \cdot V^{-1} \cdot s^{-1}$ and on/off ratios $>10^7$. Liquid-gated FETs for biosensing platforms had low voltage driving and stable behavior. Specific chemical treatment and enzyme immobilization on In_2O_3-based FET biosensors facilitated pH and glucose detection, respectively, in real-time with linear and fast responses. This ultrathin biosensor platform is advantageous as a conformal sensor *via* delamination. The devices had excellent contact on highly rough artificial skin surfaces and an artificial eye surface. We find that solution-processed metal oxide biosensors are potential candidates for further development of simple, affordable, printable, and wearable sensing technologies.

EXPERIMENTAL METHODS

Aqueous Indium Oxide Precursor Solution. Indium oxide precursor solutions were prepared at a concentration of 0.2 M by dissolving 0.3 g of indium nitrate hydrate ($In(NO_3)_3 \cdot xH_2O$) in 5 mL of deionized water. After stirring vigorously for 1 h at 30 °C, the solution appeared transparent.

Biosensor Fabrication. Substrates were sequentially cleaned in acetone and isopropyl alcohol and treated with ultraviolet (UV) irradiation for 10 min to remove organic residues and to improve solvent wettability. Indium oxide precursor solution was spin-coated on SiO_2 (1000 Å) heavily boron-doped *p*-type Si wafers or PI/glass substrates at 3000 rpm for 30 s. These substrates were then soft-baked at 100 °C for 5 min to eliminate water and annealed at 250 °C for 3 h. To evaluate the electrical performance of In_2O_3 FETs, BGTC structure was used on Si wafers (Figure 1d). The Au/Cr source and drain (S/D) electrodes (thickness = 30/10 nm) were deposited by thermal evaporation through the shadow mask. The channel region was defined with a width (*W*) of 1000 μm and a length (*L*) of 200 μm. Twenty pairs of In_2O_3 FETs were formed over an area of 1.5 × 1.5 cm.

Interdigitated electrodes (Au/Cr) were then formed using a standard photolithography process for biosensor fabrication. To prepare conformal substrates, a PI solution was spin-coated on glass substrates at 3000 rpm for 30 s. Samples were annealed in two steps: spin-coated substrates were prebaked at 140 °C for 15 min (N_2 inert gas ambient) and annealed at 250 °C in air for 1 h. The PI films were $\sim$1.5 μm thick.

Chemical Treatments for Biosensing. For pH sensing, APTES was self-assembled on indium oxide surfaces using 2% APTES by weight in toluene for 10 min. Samples were immediately cleaned using toluene. For glucose sensing, two steps were added after silanization with APTES. A glutaraldehyde linker (GD) was added to the terminal amino groups of APTES using a solution of 2.5% GD in 1× PBS for 5 min. The 1× PBS solution contained 136.8 mM NaCl, 2.7 mM KCl, 8.0 mM $Na_2HPO_4 \cdot 7H_2O$, and 0.26 mM KH_2PO_4. Samples were subsequently cleaned using 1× PBS solution to remove physically adsorbed molecules. Finally, 2 mg of glucose oxidase from *Aspergillus niger* was immobilized *via* the GD linker in 1 mL 1× PBS solution for 24 h. Various concentrations of D- and L-glucose were dissolved in 1× PBS.

Conformal Sensor Preparation and Mechanical Calculations. As-fabricated In_2O_3 semiconductors with interdigitated electrodes on PI were delaminated from the underlying glass substrates. Samples were placed in water, and the sensor/PI films were carefully peeled from the glass substrates. The PI films are hydrophobic; hence, these films float in water. Finally, samples were transferred to test substrates with rough surfaces (*i.e.*, artificial PDMS skin or an acrylic artificial eye). Theoretical calculations of adhesion energy, bending stiffness, and conformal contact thickness are detailed in the Supporting Information.

Characterization. X-ray reflectivity (XRR) measurements were performed using a Bede D1 diffractometer to calculate film densities and thicknesses. The morphology of the In_2O_3 films was investigated using atomic force microscopy (Dimension 5000 SPM, Veeco, now Bruker Nano, Santa Barbara, CA) and scanning electron microscopy (Nova 230, FEI, Hillsboro, OR). Cyclic voltammetry was used to test the redox potential of glucose using a PAR EG&G 273A potentiostat with a Ag/AgCl reference electrode and a platinum-foil counter-electrode. The measurement was performed in 1× PBS at a voltage sweep rate of 50 $mV \cdot s^{-1}$ and a potential range of 0.2−0.8 V *vs* Ag/AgCl. Electrical measurements of FET-based sensors were performed using an Agilent 4155C semiconductor analyzer (Agilent Technologies, Inc., Santa Clara, CA).

Conflict of Interest: The authors declare no competing financial interest.

Supporting Information Available: The Supporting Information is available free of charge on the ACS Publications website at DOI: 10.1021/acsnano.5b05325.

Included are leakage current measurements through the liquid-gated In_2O_3 FETs, pH-sensing results of the pristine

In_2O_3-based biosensors without APTES silanization, cyclic voltammetry of a Pt foil in 1× PBS with different glucose concentrations, and the simulation calculations of the mechanical stress values and conformal coverage over ultrathin polyimide substrates (PDF)

Acknowledgment. This work was financially supported by a grant from the National Science Foundation (Grant no. ECCS-1202231, Program Director Dr. Paul Werbos; ECCS is a program under Engineering Division), the Office of Naval Research (Program Manager Dr. Paul Armistead; Grant no. N000141410648), a grant from the CalBRAIN Neurotechnology Program, and UCLA internal funds. The authors acknowledge the use of instruments at the Nano and Pico Characterization Lab at the California NanoSystems Institute, Molecular and Nano Archaeology (MNA) Lab, and the Molecular Instrumentation Center at UCLA. We thank Dr. Hyung-Seok Kim for helpful discussions about electrochemistry.

REFERENCES AND NOTES

1. Kim, D.-H.; Viventi, J.; Amsden, J. J.; Xiao, J.; Vigeland, L.; Kim, Y. S.; Blanco, J. A.; Panilaitis, B.; Frechette, E. S.; Contreras, D.; *et al.* Dissolvable Films of Silk Fibroin for Ultrathin Conformal Bio-Integrated Electronics. *Nat. Mater.* **2010**, *9*, 511–517.
2. Kim, S. Y.; Park, S.; Park, H. W.; Park, D. H.; Jeong, Y.; Kim, D. H. Highly Sensitive and Multimodal All-Carbon Skin Sensors Capable of Simultaneously Detecting Tactile and Biological Stimuli. *Adv. Mater.* **2015**, *27*, 4105.
3. Ryu, S.; Lee, P.; Chou, J. B.; Xu, R.; Zhao, R.; Hart, A. J.; Kim, S. G. Extremely Elastic Wearable Carbon Nanotube Fiber Strain Sensor for Monitoring of Human Motion. *ACS Nano* **2015**, *9*, 5929–5936.
4. Wang, C.; Hwang, D.; Yu, Z.; Takei, K.; Park, J.; Chen, T.; Ma, B.; Javey, A. User-Interactive Electronic Skin for Instantaneous Pressure Visualization. *Nat. Mater.* **2013**, *12*, 899–904.
5. Sekitani, T.; Noguchi, Y.; Hata, K.; Fukushima, T.; Aida, T.; Someya, T. A Rubberlike Stretchable Active Matrix Using Elastic Conductors. *Science* **2008**, *321*, 1468–1472.
6. Takei, K.; Takahashi, T.; Ho, J. C.; Ko, H.; Gillies, A. G.; Leu, P. W.; Fearing, R. S.; Javey, A. Nanowire Active-Matrix Circuitry for Low-Voltage Macroscale Artificial Skin. *Nat. Mater.* **2010**, *9*, 821–826.
7. Someya, T.; Sekitani, T.; Iba, S.; Kato, Y.; Kawaguchi, H.; Sakurai, T. A Large-Area, Flexible Pressure Sensor Matrix with Organic Field-Effect Transistors for Artificial Skin Applications. *Proc. Natl. Acad. Sci. U. S. A.* **2004**, *101*, 9966–9970.
8. Mannsfeld, S. C. B.; Tee, B. C. K.; Stoltenberg, R. M.; Chen, C. V. H. H.; Barman, S.; Muir, B. V. O.; Sokolov, A. N.; Reese, C.; Bao, Z. N. Highly Sensitive Flexible Pressure Sensors with Microstructured Rubber Dielectric Layers. *Nat. Mater.* **2010**, *9*, 859–864.
9. Maheshwari, V.; Saraf, R. F. High-Resolution Thin-Film Device to Sense Texture by Touch. *Science* **2006**, *312*, 1501–1504.
10. Kim, D.-H.; Lu, N.; Ma, R.; Kim, Y. S.; Kim, R. H.; Wang, S.; Wu, J.; Won, S. M.; Tao, H.; Islam, A.; *et al.* Epidermal Electronics. *Science* **2011**, *333*, 838–843.
11. Someya, T.; Kato, Y.; Sekitani, T.; Iba, S.; Noguchi, Y.; Murase, Y.; Kawaguchi, H.; Sakurai, T. Conformable, Flexible, Large-Area Networks of Pressure and Thermal Sensors with Organic Transistor Active Matrixes. *Proc. Natl. Acad. Sci. U. S. A.* **2005**, *102*, 12321–12325.
12. Takahashi, T.; Takei, K.; Gillies, A. G.; Fearing, R. S.; Javey, A. Carbon Nanotube Active-Matrix Backplanes for Conformal Electronics and Sensors. *Nano Lett.* **2011**, *11*, 5408–5413.
13. Hammock, M. L.; Chortos, A.; Tee, B. C.; Tok, J. B.; Bao, Z. 25th Anniversary Article: The Evolution of Electronic Skin (E-Skin): A Brief History, Design Considerations, and Recent Progress. *Adv. Mater.* **2013**, *25*, 5997–6038.
14. Oklu, R.; Khademhosseini, A.; Weiss, P. S. Patient-Inspired Engineering and Nanotechnology. *ACS Nano* **2015**, *9*, 7733–7734.
15. Claussen, J. C.; Kumar, A.; Jaroch, D. B.; Khawaja, M. H.; Hibbard, A. B.; Porterfield, D. M.; Fisher, T. S. Nanostructuring Platinum Nanoparticles on Multilayered Graphene Petal Nanosheets for Electrochemical Biosensing. *Adv. Funct. Mater.* **2012**, *22*, 3399–3405.
16. Dzyadevych, S. V.; Soldatkin, A. P.; El'skaya, A. V.; Martelet, C.; Jaffrezic-Renault, N. Enzyme Biosensors Based on Ion-Selective Field-Effect Transistors. *Anal. Chim. Acta* **2006**, *568*, 248–258.
17. Zou, Y.; Xiang, C.; Sun, L. X.; Xu, F. Glucose Biosensor Based on Electrodeposition of Platinum Nanoparticles onto Carbon Nanotubes and Immobilizing Enzyme with Chitosan-SiO_2 Sol-Gel. *Biosens. Bioelectron.* **2008**, *23*, 1010–1016.
18. Cheng, Y.; Xiong, P.; Yun, C. S.; Strouse, G. F.; Zheng, J. P.; Yang, R. S.; Wang, Z. L. Mechanism and Optimization of pH Sensing Using SnO_2 Nanobelt Field Effect Transistors. *Nano Lett.* **2008**, *8*, 4179–4184.
19. Windmiller, J. R.; Wang, J. Wearable Electrochemical Sensors and Biosensors: A Review. *Electroanalysis* **2013**, *25*, 29–46.
20. Seung, W.; Gupta, M. K.; Lee, K. Y.; Shin, K. S.; Lee, J. H.; Kim, T. Y.; Kim, S.; Lin, J.; Kim, J. H.; Kim, S. W. Nanopatterned Textile-Based Wearable Triboelectric Nanogenerator. *ACS Nano* **2015**, *9*, 3501–3509.
21. Roh, E.; Hwang, B. U.; Kim, D.; Kim, B. Y.; Lee, N. E. Stretchable, Transparent, Ultrasensitive, and Patchable Strain Sensor for Human-Machine Interfaces Comprising a Nanohybrid of Carbon Nanotubes and Conductive Elastomers. *ACS Nano* **2015**, *9*, 6252–6261.
22. Ha, M.; Park, J.; Lee, Y.; Ko, H. Triboelectric Generators and Sensors for Self-Powered Wearable Electronics. *ACS Nano* **2015**, *9*, 3421–3427.
23. Choi, S.; Park, J.; Hyun, W.; Kim, J.; Kim, J.; Lee, Y. B.; Song, C.; Hwang, H. J.; Kim, J. H.; Hyeon, T.; *et al.* Stretchable Heater Using Ligand-Exchanged Silver Nanowire Nanocomposite for Wearable Articular Thermotherapy. *ACS Nano* **2015**, *9*, 6626–6633.
24. Li, C.; Lei, B.; Zhang, D.; Liu, X.; Han, S.; Tang, T.; Rouhanizadeh, M.; Hsiai, T.; Zhou, C. Chemical Gating of In_2O_3 Nanowires by Organic and Biomolecules. *Appl. Phys. Lett.* **2003**, *83*, 4014–4016.
25. Allen, B. L.; Kichambare, P. D.; Star, A. Carbon Nanotube Field-Effect-Transistor-Based Biosensors. *Adv. Mater.* **2007**, *19*, 1439–1451.
26. Chen, K.-I.; Li, B.-R.; Chen, Y.-T. Silicon Nanowire Field-Effect Transistor-Based Biosensors for Biomedical Diagnosis and Cellular Recording Investigation. *Nano Today* **2011**, *6*, 131–154.
27. Kim, J.; Rim, Y. S.; Chen, H.; Cao, H. H.; Nakatsuka, N.; Hinton, H. L.; Zhao, C.; Andrews, A. M.; Yang, Y.; Weiss, P. S. Fabrication of High-Performance Ultrathin In_2O_3 Film Field-Effect Transistors and Biosensors Using Chemical Lift-Off Lithography. *ACS Nano* **2015**, *9*, 4572–4582.
28. Torsi, L.; Tafuri, A.; Cioffi, N.; Gallazzi, M. C.; Sassella, A.; Sabbatini, L.; Zambonin, P. G. Regioregular Polythiophene Field-Effect Transistors Employed as Chemical Sensors. *Sens. Actuators, B* **2003**, *93*, 257–262.
29. Kuila, T.; Bose, S.; Khanra, P.; Mishra, A. K.; Kim, N. H.; Lee, J. H. Recent Advances in Graphene-Based Biosensors. *Biosens. Bioelectron.* **2011**, *26*, 4637–4648.
30. Sun, D. M.; Liu, C.; Ren, W. C.; Cheng, H. M. A Review of Carbon Nanotube- and Graphene-Based Flexible Thin-Film Transistors. *Small* **2013**, *9*, 1188–1205.
31. Sarkar, D.; Liu, W.; Xie, X. J.; Anselmo, A. C.; Mitragotri, S.; Banerjee, K. Correction to MoS_2 Field-Effect Transistor for Next-Generation Label-Free Biosensors. *ACS Nano* **2014**, *8*, 5367–5367.
32. Sarkar, D.; Liu, W.; Xie, X. J.; Anselmo, A. C.; Mitragotri, S.; Banerjee, K. MoS_2 Field-Effect Transistor for Next-Generation Label-Free Biosensors. *ACS Nano* **2014**, *8*, 3992–4003.
33. Hwang, B.-U.; Lee, J.-H.; Trung, T. Q.; Roh, E.; Kim, D.-I.; Kim, S.-W.; Lee, N.-E. Transparent Stretchable Self-Powered Patchable Sensor Platform with Ultrasensitive Recognition of Human Activities. *ACS Nano* **2015**, *9*, 8801–8810.

34. Rogers, J. A.; Someya, T.; Huang, Y. G. Materials and Mechanics for Stretchable Electronics. *Science* **2010**, *327*, 1603–1607.
35. Park, Y. J.; Lee, S. K.; Kim, M. S.; Kim, H.; Ahn, J. H. Graphene-Based Conformal Devices. *ACS Nano* **2014**, *8*, 7655–7662.
36. Srinivasan, C.; Mullen, T. J.; Hohman, J. N.; Anderson, M. E.; Dameron, A. A.; Andrews, A. M.; Dickey, E. C.; Horn, M. W.; Weiss, P. S. Scanning Electron Microscopy of Nanoscale Chemical Patterns. *ACS Nano* **2007**, *1*, 191–201.
37. Saavedra, H. M.; Mullen, T. J.; Zhang, P. P.; Dewey, D. C.; Claridge, S. A.; Weiss, P. S. Hybrid Strategies in Nanolithography. *Rep. Prog. Phys.* **2010**, *73*, 036501–036541.
38. Porchetta, A.; Idili, A.; Vallee-Belisle, A.; Ricci, F. General Strategy to Introduce pH-Induced Allostery in DNA-Based Receptors to Achieve Controlled Release of Ligands. *Nano Lett.* **2015**, *15*, 4467–4471.
39. Xiang, Y.; Lu, Y. Using Personal Glucose Meters and Functional DNA Sensors to Quantify a Variety of Analytical Targets. *Nat. Chem.* **2011**, *3*, 697–703.
40. Tian, K.; Prestgard, M.; Tiwari, A. A Review of Recent Advances in Nonenzymatic Glucose Sensors. *Mater. Sci. Eng., C* **2014**, *41*, 100–118.
41. Badugu, R.; Lakowicz, J. R.; Geddes, C. D. Ophthalmic Glucose Sensing: A Novel Monosaccharide Sensing Disposable and Colorless Contact Lens. *Analyst* **2004**, *129*, 516–521.
42. Neithercott, T. The Future Is Near. 14 Diabetes Products Suggest Big Things to Come. *Diabetes Forecast* **2015**, *68*, 33–35.
43. Daum, K. M.; Hill, R. M. Human Tear Glucose. *Invest. Ophthalmol. Vis. Sci.* **1982**, *22*, 509–514.
44. Rim, Y. S.; Jeong, W. H.; Kim, D. L.; Lim, H. S.; Kim, K. M.; Kim, H. J. Simultaneous Modification of Pyrolysis and Densification for Low-Temperature Solution-Processed Flexible Oxide Thin-Film Transistors. *J. Mater. Chem.* **2012**, *22*, 12491–12497.
45. Rim, Y. S.; Chen, H. J.; Kou, X. L.; Duan, H. S.; Zhou, H. P.; Cai, M.; Kim, H. J.; Yang, Y. Boost Up Mobility of Solution-Processed Metal Oxide Thin-Film Transistors *via* Confining Structure on Electron Pathways. *Adv. Mater.* **2014**, *26*, 4273–4278.
46. Chen, H.; Rim, Y. S.; Jiang, C.; Yang, Y. Low-Impurity High Performance Solution-Processed Metal Oxide Semiconductors *via* a Facile Redox Reaction. *Chem. Mater.* **2015**, *27*, 4713–4718.
47. Huang, X.; Yeo, W. H.; Liu, Y. H.; Rogers, J. A. Epidermal Differential Impedance Sensor for Conformal Skin Hydration Monitoring. *Biointerphases* **2012**, *7*, 7.
48. Opie, N. L.; Burkitt, A. N.; Meffin, H.; Grayden, D. B. Heating of the Eye by a Retinal Prosthesis: Modeling, Cadaver and *In Vivo* Study. *IEEE Trans. Biomed. Eng.* **2012**, *59*, 339–345.
49. Chaudhury, M. K.; Whitesides, G. M. Direct Measurement of Interfacial Interactions between Semispherical Lenses and Flat Sheets of Poly(dimethylsiloxane) and Their Chemical Derivatives. *Langmuir* **1991**, *7*, 1013–1025.
50. Cantarella, G.; Munzenrieder, N.; Petti, L.; Vogt, C.; Buthe, L.; Salvatore, G. A.; Daus, A.; Troster, G. Flexible In-Ga-Zn-O Thin-Film Transistors on Elastomeric Substrate Bent to 2.3% Strain. *IEEE Electron Device Lett.* **2015**, *36*, 781–783.
51. Chen, Z.; Cotterell, B.; Wang, W. The Fracture of Brittle Thin Films on Compliant Substrates in Flexible Displays. *Eng. Fract. Mech.* **2002**, *69*, 597–603.
52. Chen, Z.; Cotterell, B.; Wang, W.; Guenther, E.; Chua, S. J. A Mechanical Assessment of Flexible Optoelectronic Devices. *Thin Solid Films* **2001**, *394*, 201–205.
53. Kwak, K.; Cho, K.; Kim, S. Stable Bending Performance of Flexible Organic Light-Emitting Diodes Using IZO Anodes. *Sci. Rep.* **2013**, *3*, 2787.
54. Lin, C. Y.; Chien, C. W.; Wu, C. C.; Yeh, Y. H.; Cheng, C. C.; Lai, C. M.; Yu, M. J.; Leu, C. M.; Lee, T. M. Effects of Mechanical Strains on the Characteristics of Top-Gate Staggered a-IGZO Thin-Film Transistors Fabricated on Polyimide-Based Nanocomposite Substrates. *IEEE Trans. Electron Devices* **2012**, *59*, 1956–1962.
55. Sharma, B. K.; Jang, B.; Lee, J. E.; Bae, S. H.; Kim, T. W.; Lee, H. J.; Kim, J. H.; Ahn, J. H. Load-Controlled Roll Transfer of Oxide Transistors for Stretchable Electronics. *Adv. Funct. Mater.* **2013**, *23*, 2024–2032.
56. Cui, Y.; Wei, Q.; Park, H.; Lieber, C. M. Nanowire Nanosensors for Highly Sensitive and Selective Detection of Biological and Chemical Species. *Science* **2001**, *293*, 1289–1292.
57. Nair, P. R.; Alam, M. A. Screening-Limited Response of Nanobiosensors. *Nano Lett.* **2008**, *8*, 1281–1285.
58. Wilson, R.; Turner, A. P. F. Glucose-Oxidase - An Ideal Enzyme. *Biosens. Bioelectron.* **1992**, *7*, 165–185.
59. Bergveld, P. Thirty Years of Isfetology - What Happened in the Past 30 Years and What May Happen in the Next 30 Years. *Sens. Actuators, B* **2003**, *88*, 1–20.
60. Caras, S. D.; Janata, J.; Saupe, D.; Schmitt, K. pH-Based Enzyme Potentiometric Sensors. Part 1. Theory. *Anal. Chem.* **1985**, *57*, 1917–1920.
61. Caras, S. D.; Petelenz, D.; Janata, J. pH-Based Enzyme Potentiometric Sensors. Part 2. Glucose-Sensitive Field-Effect Transistor. *Anal. Chem.* **1985**, *57*, 1920–1923.
62. Hayek, T.; Kaplan, M.; Kerry, R.; Aviram, M. Macrophage NADPH Oxidase Activation, Impaired Cholesterol Fluxes, and Increased Cholesterol Biosynthesis in Diabetic Mice: A Stimulatory Role for D-Glucose. *Atherosclerosis* **2007**, *195*, 277–286.